Optical Materials 33 (2011) 1086–1090

Contents lists available at ScienceDirect

Optical Materials

journal homepage: www.elsevier.com/locate/optmat

Si nanoclusters coupled to Er^{3+} ions in a SiO_2 matrix for optical amplifiers

D. Navarro-Urrios [a,*], O. Jambois [a], F. Ferrarese Lupi [a], P. Pellegrino [a], B. Garrido [a], A. Pitanti [b], N. Prtljaga [b], N. Daldosso [b], L. Pavesi [b]

[a] MIND-IN2UB, Dept. Electrònica, Universitat de Barcelona, Martí i Franquès 1, 08028 Barcelona, Spain
[b] Laboratorio di Nanoscienze, Dipartimento di Fisica, Università di Trento, Via Sommarive 14, I-38100, Povo (Trento), Italy

ARTICLE INFO

Article history:
Received 7 June 2010
Received in revised form 2 December 2010
Accepted 16 December 2010
Available online 8 January 2011

Keywords:
Si nanoclusters
Erbium
Energy transfer
Optical amplifier

ABSTRACT

In this work we will give an overview of the optical properties of Si nanoclusters coupled to Er^{3+} ions in SiO_2 matrices produced by reactive magnetron co-sputtering. We have divided the work into two separate studies realised on the same samples, which are the result of a thorough optimisation work. The first one have been realised in order to get a clear picture of the interaction mechanism. On the second we will show a quantitative evaluation of the potential performances from a material point of view (determination of the whole optically active Er^{3+} content, excitable by direct or indirect means) and actual performance in a waveguide device (determination of internal gain values).

1. Introduction

One of the scientific and technological challenges of silicon-based photonics consists in making silicon an efficient light emitter, eventually also providing amplification. This will allow combining both the functionality of silicon microelectronics with ultra-fast optical data generation, processing and transmission on a single silicon-based device.

Low dimensional silicon in the form of silicon nanoclusters (Si-nc) is a material with extremely interesting optoelectronic properties that differ strongly from those of bulk Si. In particular, the capacity of Si-nc to act as sensitizers of rare earth ions, specifically erbium ions (Er^{3+}) [1], has opened the route towards an all-optical light Si based amplifiers operating in the third telecommunication window. However, during the last years, several reports have shown what seems to be an intrinsic limit of the material itself, as to say. the low amount of Er^{3+} taking advantage of an efficient indirect transfer mechanism [2–5]. The fundamental reason of the low excitable percentage is still under debate and a number of different issues have been proposed as final limiting factors. Among them, the most extended ones have been the finite interaction distance of the coupling strength [4], the presence of Auger back-transfer mechanisms [5], excited state absorption processes [6] cooperative up-conversion [3] and the limited concentration of Er^{3+} ions able to emit light [7].

The study presented here is crucial for the understanding and optimisation of the performances of this material, which has been in this case fabricated by reactive magnetron co-sputtering.

In the first part of the paper we will show a modelling of the transfer mechanism through a set of coupled rate equations involving the carrier populations of a number of effective levels within the Si-nc and the Er^{3+} ions. This model includes several recombination and excitation mechanisms, well grounded on the basis of several evidences observed in continuous wave and time-resolved photoluminescence measurements. We will address afterwards the issue of quantifying of the different concentrations that determine the potentiality of the material for light amplification, as to say: (i) the total content of erbium present in the material, (ii) the concentration of Er^{3+} ions that are absorbing light, (iii) the concentration of the ones that are optically active and emit light, (iv) the concentration of the ones that are efficiently coupled to the Si-nc and emit light.

Finally, the characterisation will be addressed of waveguide devices that quantify absolute values of absorption losses and gain.

2. Experimental

The samples under study have been fabricated by a RF reactive magnetron co-sputtering under Argon–Hydrogen mixture of 2-in. confocal pure SiO_2 and Er_2O_3 targets [8]. To form nanoparticles, a substoichiometric Silicon Rich Silicon Oxide (SRSO) has been deposited followed by an annealing treatment to promote phase separation between silicon and its oxide. In order to perform comparative spectroscopic characterisation, the deposition parameters

* Corresponding author.
E-mail address: dnavarro@el.ub.es (D. Navarro-Urrios).

0925-3467/$ - see front matter © 2010 Elsevier B.V. All rights reserved.
doi:10.1016/j.optmat.2010.12.003

employed to obtain the best sample in terms of high PhotoLuminescence (PL) intensity (under non-resonant pumping – 476 nm) and long lifetime of the $^4I_{13/2} \rightarrow {}^4I_{15/2}$ Er^{3+} transition, have been used to fabricate a set of different samples with and without Er^{3+} and with different annealing treatments.

Here we will report about two samples deposited over a 5 μm-SiO_2 cladding layer above a Si substrate: sample A (Si excess of 5%, Er^{3+} content of 3.4×10^{20} cm^{-3}, and thickness 1.2 μm) and sample B (same deposition conditions but without Er^{3+}). Both layers were annealed at 910 °C during 60 min under a pure nitrogen flow, so they likely contain Si in an amorphous nanocluster form [8]. Some of the measurements shown in this paper were done on rib-loaded waveguides, which have been formed by dry etching the slab waveguides [9].

The spectroscopic experiments have been performed both in visible (VIS) and near-infrared (IR) range, with Continuous-Wave (CW) and pulsed laser excitation sources. The CW source was an Ar^+ laser of which we have employed lines which were resonant (488 nm) or non-resonant (476 nm) with Er^{3+} internal transitions.

The pulsed source was the third harmonic (355 nm) of a Nd:YAG laser with 10 ns pulse width, a repetition rate of 10 Hz and a photon flux of 1×10^{25} ph/(cm^2 s) during the pulse. For detection in the visible we have used a CCD streak camera coupled to a spectrometer, with an overall time-resolution of the order of few picoseconds, and a monochromator coupled with a GaAs-PhotoMulTiplier (PMT), respectively for Time Resolved (TR) and CW measurements. In the infrared, the signal was spectrally resolved with a monochromator and subsequently detected with a InGaAs IR-PMT. All measurements have been performed at room temperature.

3. Results

A typical PL spectrum of our samples, measured with an excitation wavelength non-resonant with any Er^{3+} internal transition (476 nm), is shown in Fig. 1. It is possible to recognize several spectral features: around 980 nm and 1535 nm, the characteristic transitions of Er^{3+} in SiO_2 appear, related respectively to the first and second excited to the fundamental state optical transitions. The wide band centred at around 700 nm is related to Si-nc emission, while the emission band at about 1100 nm is due to the Si substrate. In the right panels of the same figure we present separately the temporal decay of the PL signals after a fast (10 ns) pulsed excitation at 355 nm for the IR transitions (top right), related to Er^{3+} emission, and for the VIS transitions (bottom right), related to Si-nc emission.

The analysis of the IR emission reveals that the signal at 0.98 μm ($^4I_{11/2} \rightarrow {}^4I_{15/2}$ transition) after a steep rise that lasts less than 100 ns is constantly decreasing as a single exponential function, with a time constant of 4.6 ± 0.5 μs. On the other hand, the 1.535 μm signal ($^4I_{13/2} \rightarrow {}^4I_{15/2}$ transition) is rising with almost the same time constant (4.2 ± 0.5 μs). It is not possible to compare directly the populations in the two levels, since the PL intensities are inversely proportional to the unknown radiative lifetimes. However, it is clear that the 1.535 μm signal never rises above the 0.98 μm one, implying that a great part of the energy transfer process involves the level $^4I_{11/2}$ and that the level $^4I_{13/2}$ is populated mainly through internal relaxation processes. A fast transfer process that populates directly the $^4I_{13/2}$ level could be also present, though its impact would be at most of the same magnitude than the transfer to the $^4I_{11/2}$ level. It is not possible to exactly quantify its contribution since the first nanoseconds of PL dynamics are hidden by a fast decaying emission that will be discussed hereafter.

The single exponential function observed in the 0.98 μm decay suggests that no level energetically higher than $^4I_{11/2}$ is excited during the transfer process, since otherwise the $^4I_{11/2}$ would be repopulated during the decay, at least during the first tens of ns. This is further supported by the absence of visible PL emission involving transitions from higher energy levels.

One of the most striking features is the appearance of a very fast (tens of ns) signal, already mentioned in the previous discussion. A similar component was observed by other authors and was associated to Auger back-transfer mechanisms from excited Er^{3+} to excited carriers within the Si-nc [5], however it covers a very broad spectral range, i.e. not only where Er^{3+} transitions are present [10,11]. Moreover, the same kind of fast component is present also for sample B, whose intensity of the visible PL is quenched by roughly the same factor when erbium is inserted in the sample (see next paragraphs). Its origin could be attributed to radiative

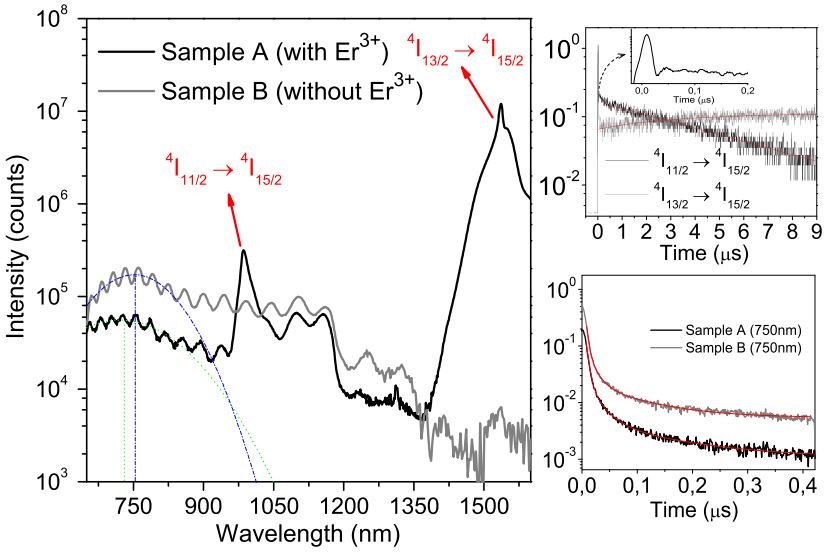

Fig. 1. PL emission from sample A (black) and B (gray). Gaussian fits to the Si-nc associated emission have been included. The top right panel shows a comparison of $^4I_{11/2} \rightarrow {}^4I_{15/2}$ and $^4I_{13/2} \rightarrow {}^4I_{15/2}$ PL temporal behaviours after the pump pulse in sample A. In red, the simulation results using the model presented in this manuscript are reported, holding a decay time of 4.6 ± 0.5 μs (980 nm signal) and a rise time of 4.2 ± 0.5 μs (1535 nm signal). A zoom of the first 200 ns for the PL associated to the $^4I_{11/2} \rightarrow {}^4I_{15/2}$ has been also included. The bottom right panel shows the experimental and simulated (red curves) PL decays of the visible signal (0.65–0.95 μm). (For interpretation of the references to color in this figure legend, the reader is referred to the web version of this article.)